Inclusive neutrino and antineutrino scattering within the coherent density fluctuation model

Martin Ivanov[1,2,*] and *Anton* Antonov[1,**]

[1]Institute for Nuclear Research and Nuclear Energy, Bulgarian Academy of Sciences, 1784 Sofia, Bulgaria
[2]Department of Physics, Faculty of Mathematics and Natural Sciences, South-West University "Neofit Rilski", Blagoevgrad, Bulgaria

Abstract. The experimental data from quasielastic neutrino and antineutrino scattering on ^{12}C are analyzed in terms of a new scaling variable ψ^* suggested by the interacting relativistic Fermi gas model with scalar and vector interactions, which is known to generate a relativistic effective mass for the interacting nucleons. We construct a new scaling function $f^{\rm QE}(\psi^*)$ for the inclusive lepton scattering from nuclei within the coherent density fluctuation model (CDFM). The latter is a natural extension of the relativistic Fermi gas (RFG) model to finite nuclei. In this work, on the basis of the scaling function obtained within CDFM with a relativistic effective mass m_N^* from $0.6m_N$ to $1.0m_N$, thus demonstrating its role in more details, we calculate and compare the theoretical predictions with a large set of experimental data for inclusive (anti)neutrino cross sections. The model also includes the contribution of weak two-body currents in the two-particle two-hole sector, evaluated within a fully RFG. Good agreement with experimental data is found over the whole range (anti)neutrino energies.

1 Introduction

The superscaling approach (SuSA) [1–6] relies on the superscaling properties of the electron scattering data: at sufficiently high momentum transfer the inclusive differential (e, e') cross sections, divided by a suitable function which takes into account the single nucleon content of the problem:

$$f = \frac{d^2\sigma/d\Omega dk'}{S(q,\omega)}, \tag{1}$$

depend only upon one kinematical variable (this behavior is called scaling of first kind) and the resulting function is approximately the same for all nuclei (scaling of second kind). When both kinds of scaling are fulfilled the cross section is said to superscale.

The superscaling phenomenon was firstly considered within the framework of the Relativistic Fermi Gas (RFG) model, where a properly defined function of the scaling ψ-variable was introduced. It was observed that the experimental data have a superscaling behavior in the low-ω side (ω being the transfer energy) of the quasielastic peak for large negative values of ψ (up to $\psi \approx -2$), while the predictions of the RFG model are $f(\psi) = 0$ for $\psi \leq -1$. This imposes the consideration of the superscaling in realistic finite systems. One of the approaches to do this was developed [7, 8] in the CDFM [9–16] which is related to the δ-function limit of the generator coordinate method [7, 17]. It was shown in [7, 8, 18] that the superscaling in nuclei can be explained quantitatively on the basis of the similar behavior of the high-momentum components of the nucleon momentum distribution in light, medium and heavy nuclei. It is well known that the latter is related to the effects of the *NN* correlations in nuclei (see, *e.g.* [9, 10]).

In our previous works [7, 8, 18, 19] we obtained the CDFM scaling function $f(\psi)$ starting from the RFG model scaling function $f_{\rm RFG}(\psi)$ and convoluting it with the weight function $|F(x)|^2$ that is related equivalently to either the density $\rho(r)$ or the nucleon momentum distribution $n(k)$ in nuclei. Thus, the CDFM scaling function is an infinite superposition of weighted RFG scaling functions. This approach improves upon RFG and enables one to describe the scaling function for realistic finite nuclear systems. The CDFM scaling function has been used to predict cross sections for several processes such as the inclusive electron scattering in the QE and Δ- regions [19, 20] and neutrino (antineutrino) scattering both for charge-changing (CC) [20] and for neutral-current (NC) [21] processes.

In a recently published paper [22] we have investigated and developed a new scaling approach CDFM$_{M^*}$ (CDFM with effective mass m_N^* and $M^* = m_N^*/m_N$) using the scaling function derived in the CDFM, the latter being based on the scaling function of the relativistic Fermi gas. We use also a new scaling variable ψ^* extracted from the scaling properties of the Relativistic Mean Field (RMF) model in nuclear matter [23]. The new scaling function $f^*(\psi^*)$ including dynamical relativistic effects [23–27] is introduced through an effective mass into its definition. Within the CDFM$_{M^*}$ model we have obtained a scaling function $f^{\rm QE}(\psi^*)$ in the QE-region using the empirical density distribution of protons to determine the weight func-

*e-mail: martin@inrne.bas.bg
**e-mail: antonovshumen@gmail.com

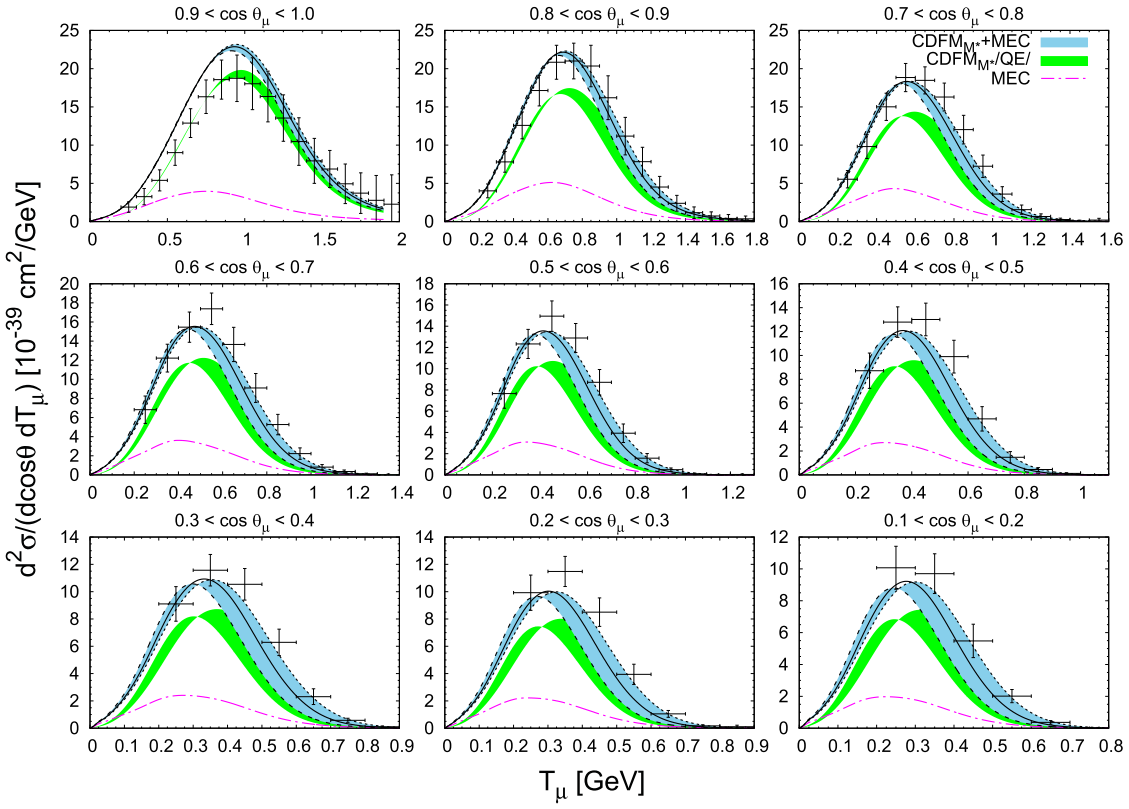

Figure 1. (Color online) MiniBooNE flux-folded double differential cross section per target neutron for the ν_μ CCQE process on ^{12}C displayed versus the μ^- kinetic energy T_μ for various bins of $\cos\theta_\mu$ obtained within the CDFM$_{M^*}$ model including MEC. 2p–2h MEC and QE (obtained within the CDFM$_{M^*}$ model for $M^* = 0.6 \div 1.0$) results are shown separately. The green shaded area presents QE results obtained within the CDFM$_{M^*}$ model with $M^* = 0.6 \div 1.0$, while the blue shaded band shows the CDFM$_{M^*}$ model including MEC. The data are from [29].

tion $|F(x)|^2$. The Fermi momentum k_F in the CDFM$_{M^*}$ model is not a free parameter. With the scaling function $f^{\rm QE}(\psi^*)$ we calculated the longitudinal and transverse response functions in both ways: using the scaling function from the CDFM$_{M^*}$ and also with the conventional scaling function of the CDFM model (CDFM$_{M^*}$ model with $M^* = 1$). The CDFM$_{M^*}$ model shows the enhancement of the transverse components of the electromagnetic current. This confirms that using the effective nucleon mass reduction of $M^* = 0.8$ leads to the enhancement of the transverse response (the RMF model includes some dynamical relativistic effects like enhancement of the transverse response due to the lower components of the nucleon spinors). We computed the inclusive (e, e') and (anti)neutrino differential quasielastic cross section with scaling function $f^{\rm QE}(\psi^*)$, adding the 2p-2h MEC contribution obtained within the RFG model to the QE results. It is found a reasonable description of the electron [28] and (anti)neutrino MiniBooNE [29, 30] data.

In the present work we use the CDFM$_{M^*}$ approach to investigate the (anti)neutrino–nuclei CC processes calculating quasielastic cross sections for different values of $M^* = 0.6 \div 1.0$ and compare the results with the data from the MiniBooNE experiment. The model also includes the contribution of weak two-body currents in the two-particle two-hole sector, evaluated within a fully relativistic Fermi gas. In Section 2, we present our main results. Finally, in Section 3, we draw conclusions of the present work.

2 Results and discussions

In this section we use the new scaling function of the CDFM$_{M^*}$ model (see Ref. [22]) to compute neutrino and antineutrino scattering cross sections on ^{12}C. In Figs. 1 and 2 are shown the double differential cross section averaged over the neutrino and antineutrino energy flux against the kinetic energy of the final muon. The data are taken from the MiniBooNE Collaboration [29, 30]. We represent a large variety of kinematical situations where each panel refers to results averaged over a particular muon angular bin. The green shaded area presents QE results obtained within the CDFM$_{M^*}$ model with $M^* = 0.6 \div 1.0$, while the blue shaded band shows the CDFM$_{M^*}$ model including MEC. The results with $M^* = 0.6$, 0.8, and 1.0 are represented by dashed, solid, and dotted black lines, respectively.

In this work we make use of the 2p-2h MEC model developed in Ref. [32], which is an extension to the weak sector of the seminal papers [33–35] for the electromagnetic case. The calculation is entirely based on the RFG model and it incorporates the explicit evaluation of the five response functions involved in inclusive neutrino scattering. We use a general parametrization of the MEC re-

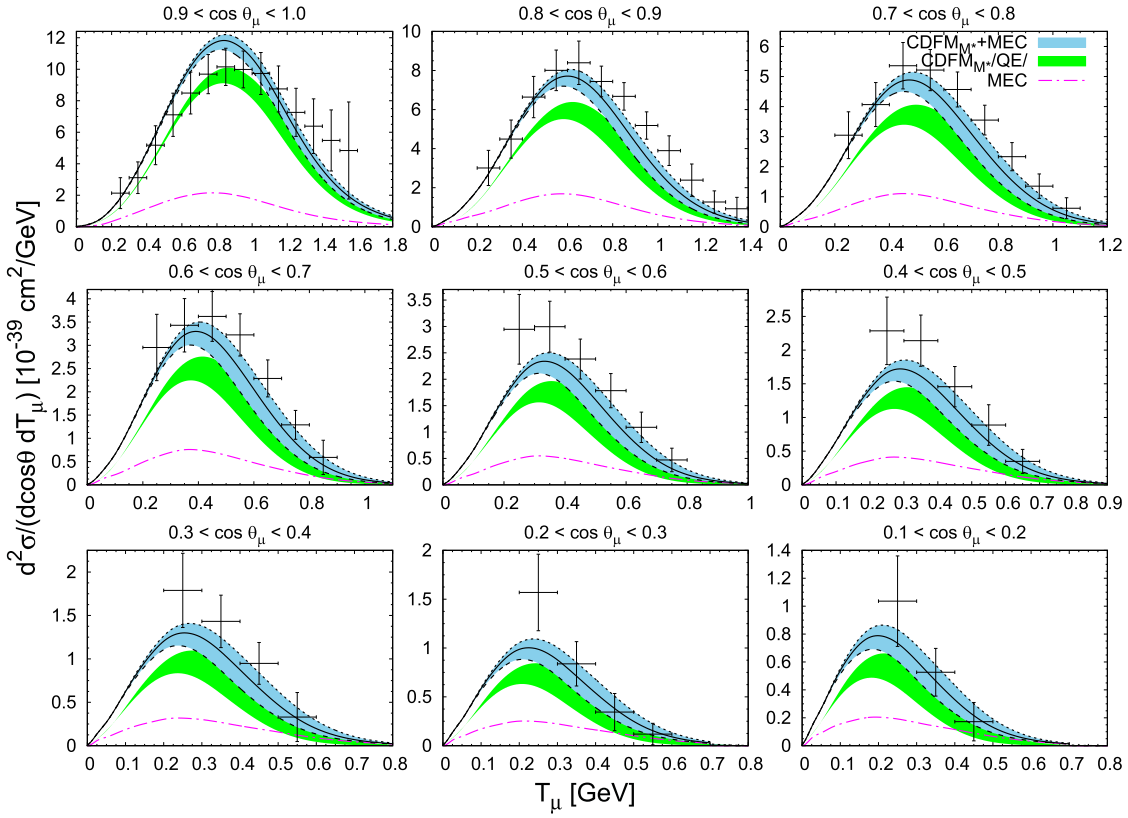

Figure 2. (Color online) As for Fig. 1, but now for the $\overline{\nu}_\mu$ CCQE process on ^{12}C. The data are from [30].

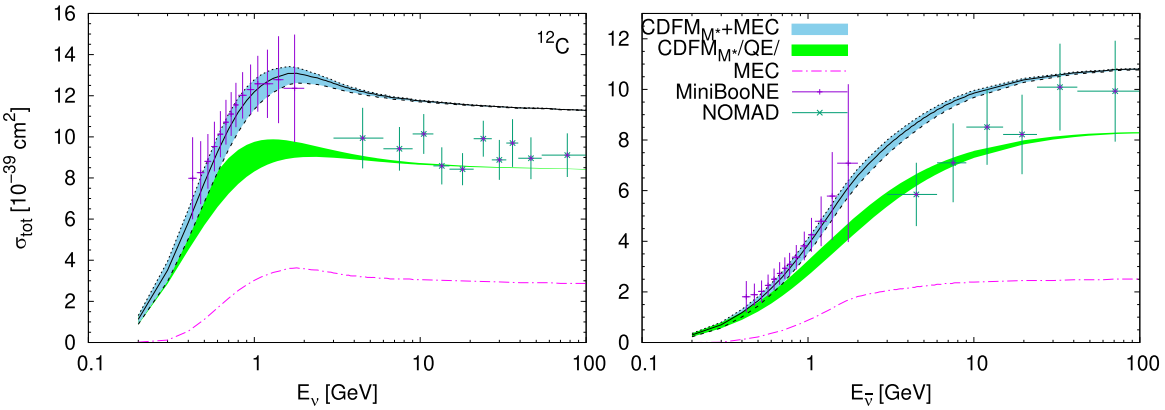

Figure 3. (Color online) CCQE ν_μ–^{12}C ($\overline{\nu}_\mu$–^{12}C) total cross section per neutron (proton) as a function of the neutrino energy. The left panel corresponds to neutrino cross sections and the right one to antineutrino reactions. The data are from MiniBooNE [29, 30] and NOMAD [31] experiments.

sponses that significantly reduces the computational time. Its functional form for the cases of ^{12}C and ^{16}O is given in Refs. [36–38].

The results including both QE (obtained within the CDFM$_{M^*}$ model with $M^* = 0.6 \div 1.0$) and 2p–2h MEC are compared with the data in Figs. 1 and 2. The QE and 2p–2h MEC contributions are presented separately also in the figures. It should be noted the important role played by 2p-2h MEC to describe correctly the experimental data of the order of ∼20–25% of the total response at the maximum. In the neutrino case (Fig. 1) this relative strength is almost independent of the scattering angle. In the antineutrino case (Fig. 2) the 2p-2h relative strength gets larger for backward scattering angles. This is due to the fact that the antineutrino cross section involves a destructive interference between the T and T' channels and is therefore more sensitive to nuclear effects.

In Ref. [22] we present CCQE results with $M^* = 0.8$ which in the present work are given by black solid line. Here we extend our analysis using also additional values of $M^* = 0.6 \div 1.0$. In the case of $M^* = 1.0$ the results are given by dotted black line and correspond to the one of the conventional CDFM model. The theoretical predictions within the CDFM$_{M^*}$ model including both QE

(with $M^* = 0.6 \div 1.0$) and 2p-2h MEC contributions are in good agreement with the data in most of the kinematical situations explored. It is important to point out that in our work [19] we reproduce experimental data of the inclusive electron scattering in the QE-region using CDFM scaling function which is obtained by the parametrizing the RFG scaling function and by the coefficient c_1, which helps us to account for the experimental fact of the asymmetry of the scaling function. The value of the coefficient c_1 ($c_1 \neq 3/4$) is taken in accordance with the empirical data (c_1 depends on the value of the momentum transfer in the QE peak). On the contrary, in Ref. [22], by using just one fixed parameter $M^* = 0.8$ due to the enhanced transverse response, we successfully reproduced experimental data of inclusive electron scattering. In the present study we demonstrate the role of the parameter M^* in the (anti)neutrino CCQE scattering cross sections. This role can be summarized as follows: with a decrease in M^*, the QE peak shifts to lower values of the muon kinetic energy T_μ, and the maximum of the QE peak decreases. Additionally, as shown in Figs. 1 and 2, the role of M^* is significantly larger on right side of the QE peak than on the left side.

The CDFM$_{M^*}$ results for the total flux-unfolded integrated cross sections per nucleon are given in Fig. 3 being compared with the MiniBooNE [29, 30] and NOMAD [31] data (up to 100 GeV). As can be seen in Fig 3, the 2p-2h MEC contributions are needed in order to reproduce the MiniBooNE data. The CDFM$_{M^*}$ model with 2p–2h MEC clearly overpredicts the NOMAD data. On the contrary, the results without MEC contributions (the pure QE results obtained within CDFM$_{M^*}$ model) are in good agreement with the NOMAD data. This result is consistent with the setup of the NOMAD experiment that, unlike MiniBooNE, can select true QE, rather than the "QE-like" events. The role of the 2p-2h MEC is very important at all neutrino energies, getting an almost constant value of the order of $\sim 30\% - 35\%$ compared with the pure QE contribution.

3 Conclusions

It is shown in our work that the CDFM$_{M^*}$ model describes successfully inclusive $\nu(\overline{\nu})$ CCQE cross section on the basis of the new scaling variable ψ^*, of the empirical density distribution of protons to determine the weight function $|F(x)|^2$, and of the corresponding scaling function $f^{\rm QE}(\psi^*)$. We analyze the role of the effective mass $M^* = m_N^*/m_N = 0.6 \div 1.0$ on the inclusive $\nu(\bar{\nu})$ CCQE cross sections. The effective mass is originating from the interacting RFG model in which the vector and scalar potentials generate the effective mass of the nucleon in medium. We should emphasize that the CDFM$_{M^*}$ scaling function keeps the gauge invariance (that is not the case in the SuSA approach) and describes the dynamical enhancement of the lower components of the relativistic spinors, as well as the transverse response function. In addition, we note the important fact that in the CDFM$_{M^*}$ model the weight and scaling functions are normalized to unity. It is pointed out that the constructed realistic CDFM$_{M^*}$ scaling function is an essential ingredient in this approach for the description of the processes of lepton scattering from nuclei.

References

[1] W.M. Alberico et al., Phys. Rev. C **38**, 1801 (1988).
[2] M. Barbaro et al., Nucl. Phys. A **643**, 137 (1998).
[3] T.W. Donnelly, I. Sick, Phys. Rev. Lett. **82**, 3212 (1999).
[4] T.W. Donnelly, I. Sick, Phys. Rev. C **60**, 065502 (1999).
[5] C. Maieron et al., Phys. Rev. C **65**, 025502 (2002).
[6] M.B. Barbaro et al., Phys. Rev. C **69**, 035502 (2004).
[7] A.N. Antonov et al., Phys. Rev. C **69**, 044321 (2004).
[8] A.N. Antonov et al., Phys. Rev. C **71**, 014317 (2005).
[9] A.N. Antonov, P.E. Hodgson, I.Z. Petkov, Nucleon Momentum and Density Distributions in Nuclei (Clarendon Press, Oxford, 1988), ISBN 9780198517269
[10] A.N. Antonov, P.E. Hodgson, I.Z. Petkov, Nucleon Correlations in Nuclei (Springer-Verlag, Berlin-Heidelberg-New York, 1993), ISBN 9783642777684
[11] A.N. Antonov et al., Bulg. J. Phys. **6**, 151 (1979).
[12] A.N. Antonov et al., Z. Phys. A **297**, 257 (1980).
[13] A.N. Antonov et al., Z. Phys. A **304**, 239 (1982).
[14] A.N. Antonov et al., Nuovo Cimento A **86**, 23 (1985).
[15] A.N. Antonov et al., Nuovo Cimento A **102**, 1701 (1989).
[16] A.N. Antonov et al., Phys. Rev. C **50**, 164 (1994).
[17] J.J. Griffin et al., Phys. Rev. **108**, 311 (1957).
[18] A.N. Antonov et al., Phys. Rev. C **73**, 047302 (2006).
[19] A.N. Antonov et al., Phys. Rev. C **74**, 054603 (2006).
[20] M.V. Ivanov et al., Phys. Rev. C **77**, 034612 (2008).
[21] A.N. Antonov et al., Phys. Rev. C **75**, 064617 (2007).
[22] M.V. Ivanov et al., Phys. Rev. C **109**, 064621 (2024).
[23] J.E. Amaro et al., Phys. Rev. C **92**, 054607 (2015).
[24] J.E. Amaro et al., Phys. Rev. D **95**, 076009 (2017).
[25] V.L. Martinez-Consentino et al., Phys. Rev. C **96**, 064612 (2017).
[26] J.E. Amaro et al., Phys. Rev. C **98**, 024627 (2018).
[27] I. Ruiz Simo et al., Phys. Rev. D **97**, 116006 (2018).
[28] O. Benhar et al., Rev. Mod. Phys. **80**, 189 (2008).
[29] A. Aguilar-Arevalo et al. (MiniBooNE Collaboration), Phys. Rev. D **81**, 092005 (2010).
[30] A.A. Aguilar-Arevalo et al. (MiniBooNE Collaboration), Phys. Rev. D **88**, 032001 (2013).
[31] V. Lyubushkin et al. (NOMAD Collaboration), Eur. Phys. J. C **63**, 355 (2009).
[32] I. Ruiz Simo et al., J. Phys. G **44**, 065105 (2017).
[33] J.W. Van Orden et al., Annals Phys. **131**, 451 (1981).
[34] A. De Pace et al., Nucl. Phys. A **726**, 303 (2003).
[35] J.E. Amaro et al., Phys. Rev. C **82**, 044601 (2010).
[36] G.D. Megias et al., Phys. Rev. D **94**, 093004 (2016).
[37] G.D. Megias et al., Phys. Rev. D **94**, 013012 (2016).
[38] G.D. Megias et al., J. Phys. G **46**, 015104 (2018).